Testing of the Taylor Frozen-in-flow Hypothesis at Electron Scales in the Solar Wind Turbulence

S. Huang, Fouad Sahraoui

▶ **To cite this version:**

S. Huang, Fouad Sahraoui. Testing of the Taylor Frozen-in-flow Hypothesis at Electron Scales in the Solar Wind Turbulence. The Astrophysical Journal Letters, 2019, 876 (2), pp.138. ⟨10.3847/1538-4357/ab17d3⟩. ⟨hal-02147138⟩

HAL Id: hal-02147138

https://hal.sorbonne-universite.fr/hal-02147138v1

Submitted on 4 Jun 2019

HAL is a multi-disciplinary open access archive for the deposit and dissemination of scientific research documents, whether they are published or not. The documents may come from teaching and research institutions in France or abroad, or from public or private research centers.

L'archive ouverte pluridisciplinaire **HAL**, est destinée au dépôt et à la diffusion de documents scientifiques de niveau recherche, publiés ou non, émanant des établissements d'enseignement et de recherche français ou étrangers, des laboratoires publics ou privés.

HAL Authorization

The Astrophysical Journal, 876:138 (7pp), 2019 May 10 https://doi.org/10.3847/1538-4357/ab17d3
© 2019. The American Astronomical Society.
OPEN ACCESS

Testing of the Taylor Frozen-in-flow Hypothesis at Electron Scales in the Solar Wind Turbulence

S. Y. Huang[1] and F. Sahraoui[2]
[1] School of Electronic Information, Wuhan University, Wuhan, People's Republic of China; shiyonghuang@whu.edu.cn
[2] Laboratoire de Physique des Plasmas, CNRS-Ecole Polytechnique-UPMC, Palaiseau, France
Received 2016 August 7; revised 2019 April 4; accepted 2019 April 8; published 2019 May 14

Abstract

In single-spacecraft observations the Taylor frozen-in-flow hypothesis is usually used to infer wavenumber spectra of turbulence from the frequency ones. While this hypothesis can be valid at MHD scales in the solar wind because of the small phase speeds of the fluctuations in comparison with the solar wind flow speed, its validity at electron scales is questionable. In this paper, we use *Cluster* data to verify the validity of the Taylor hypothesis in solar wind turbulence using the test proposed in Sahraoui et al. based on the assumption that the spectral breaks occur at ρ_i and ρ_e. Using a model based on the dispersion relation of the linear whistler mode and the estimated ratios of the spectral breaks of the magnetic energy observed in the free-streaming solar wind, we find that 32% of the events would violate the Taylor hypothesis because of their high frequency (in the plasma rest frame) compared to the Doppler shift $\boldsymbol{k}\cdot\boldsymbol{V}(|\omega_{plas}/k\cdot V| > 0.5)$. Furthermore, the model shows that those events would correspond to whistler modes with propagation angles $\theta_{kB} \leqslant 68°$. The limitations of the method used and the implications of the results on future spacecraft measurements of electron-scale turbulence are discussed.

Key words: solar wind – Sun: heliosphere – Sun: magnetic fields – waves

1. Introduction

In the solar wind, high-time-resolution electric and magnetic field observations from different spacecraft such as *Stereo*, *Cluster,* and *THEMIS* provide good opportunities to investigate turbulence cascades from magnetohydrodynamic (MHD) scales down to electron scales (e.g., Kiyani et al. 2009, 2015, Sahraoui et al. 2009, 2010a; 2013, Alexandrova et al. 2012; Salem et al. 2012; Chen et al. 2013). Nevertheless, a longstanding problem in analyzing single-spacecraft observations is the so-called spatio-temporal ambiguity, i.e., the difficulty of separating space and time variations, which are entangled in the measured data on board spacecraft. More specifically, in turbulence studies the difficulty is inferring the wavenumber spectra, which are generally predicted by turbulence theories, from the frequency spectra measured on board spacecraft. Indeed, the general formula relating the observed frequency on board the spacecraft ω_{sc} to the corresponding one in the plasma rest frame ω_{plas} is given by

$$\omega_{sc} = \omega_{plas} + \boldsymbol{k}\cdot\boldsymbol{V} = \omega_{plas} + kV\cos\theta_{kV}, \quad (1)$$

where θ_{kV} is the angle between the wave vector $\boldsymbol{k}$ and the solar wind flow $\boldsymbol{V}$. To unambiguously determine ω_{plas} it is necessary to estimate the $\boldsymbol{k}$-spectrum at each observed frequency ω_{sc}, which requires using multi-spacecraft data and appropriate techniques such as the k-filtering technique (e.g., Sahraoui et al. 2003, 2010a, 2010b, Tjulin et al. 2005; Huang et al. 2010, 2012; Narita et al. 2010).[3] Due to the supersonic and super-Alfvénic nature of the solar wind, the Taylor hypothesis is often used to derive wavenumber spectra along the plasma flow direction from the observed ones in the spacecraft frame ($\omega_{plas} \ll \boldsymbol{k}\cdot\boldsymbol{V} \Rightarrow \omega_{sc} \sim \boldsymbol{k}\cdot\boldsymbol{V} = kV\cos\theta_{kV}$). While this assumption is likely to be valid at MHD scales, it may totally fail at electron scales where dispersive modes that have phase speeds comparable or higher than the flow speed V_f may exist, e.g., the quasi-parallel whistler (Lacombe et al. 2014). Despite this limitation, and given that no multi-spacecraft mission with separation of the order of the electron scale (~1 km) exists so far, the Taylor hypothesis has been also applied to sub-ion and electron scales (e.g., Bale et al. 2005; Sahraoui et al. 2009; Alexandrova et al. 2012; Kiyani et al. 2013). At those scales only stationary structures or very-low-frequency fluctuations such as high oblique kinetic Alfvén waves (KAWs) can fulfill the Taylor hypothesis (e.g., Saito et al. 2010; Sahraoui et al. 2012; Howes et al. 2014; Zhao et al. 2014; Chen & Boldyrev 2017).

In the absence of multi-spacecraft data that would allow us to unambiguously identify the nature of the plasma modes carrying the turbulence cascade at electron scales, it is important to develop alternative tests of the Taylor hypothesis. Such a test was proposed in Sahraoui et al. (2012), based upon estimating the ratio between the ion and electron break frequencies observed on the magnetic field spectra measured on board the spacecraft. This test is recalled below.

2. Methodology

2.1. Taylor Hypothesis Test Method

Spacecraft observations in the solar wind showed that the power spectral densities (PSDs) of the magnetic fluctuations in the frequency range ~$[10^{-3}, 10^{2}]$ Hz generally have three ranges of scales with different slopes separated by two breakpoints occurring around the ion and the electron gyroscale

[3] In fact, estimating ω_{plas} requires only measuring one component of the $\boldsymbol{k}$-vector, namely the component parallel to the flow $\boldsymbol{V}$. However, once ω_{plas} is determined the full $\boldsymbol{k}$-vector is needed to determine 3D dispersion relations, i.e., $\omega_{plas} = \omega_{plas}(\boldsymbol{k})$.

Original content from this work may be used under the terms of the Creative Commons Attribution 3.0 licence. Any further distribution of this work must maintain attribution to the author(s) and the title of the work, journal citation and DOI.

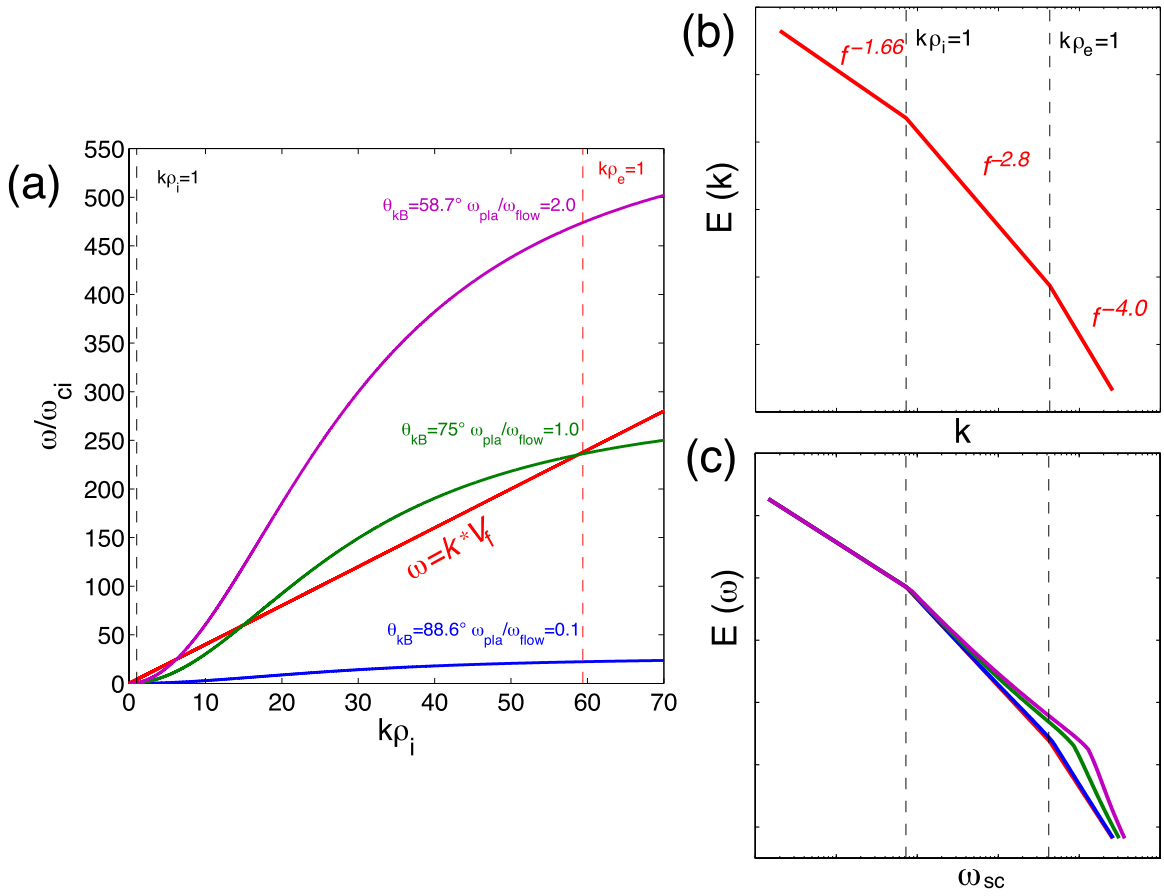

Figure 1. (a) Dispersion relations of whistler modes for three different propagation angles: 88.°6 (blue curve), 75° (green curve), and 58.°7 (magenta curve), which correspond to the values 0.1, 1.0, and 2.0 of $\omega_{\rm pla}/\omega_{\rm flow}$ at $\rho_{\rm e}$ (see the text); the red line is the Doppler curve $\omega = \boldsymbol{k}\cdot\boldsymbol{V}_{\rm f}$. (b) A simulated power-law wavenumber spectrum with slopes of -1.66 in the inertial range, -2.8 between $\rho_{\rm i}$ and $\rho_{\rm e}$, and -4.0 below $\rho_{\rm e}$. (c) The resulting spectra in the spacecraft frame using Equation (1) (see the text) and the linear solutions given in (a). The same color code applies. The power spectral density is conserved when transforming from the plasma to the spacecraft and frames. The two dashed vertical lines correspond to the frequencies resulting from Taylor-shifting the scales $\rho_{\rm i}$ and $\rho_{\rm e}$ in (c).

scales $\rho_{\rm i}$ and $\rho_{\rm e}$ (e.g., Kiyani et al. 2009, 2015, Sahraoui et al. 2009, 2010a, 2013, Huang et al. 2012, 2014, 2017). Based on the observational results, Sahraoui et al. (2012) proposed a simple test to check the validity of the Taylor hypothesis. Here, we recall briefly its principle. Let us assume that two breakpoints occur in the turbulence energy spectra at the ion and electron gyroscales in the plasma rest frame and that these two breaks are observed at the frequencies $f_{\rm bi}$ and $f_{\rm be}$ on board the spacecraft (the letter "b" stands for "break"), as illustrated in Figures 1(b) and (c). If the Taylor hypothesis is valid, then these break frequencies should correspond to the frequencies resulting from Taylor-shifting the scales $\rho_{\rm i}$ and $\rho_{\rm e}$, namely: $f_{\rm bi} \sim f_{\rho{\rm i}} = V\ \cos\theta_{kV}/2\pi\rho_{\rm i}$ and $f_{\rm be} \sim f_{\rho{\rm e}} = V\ \cos\theta_{kV}/2\pi\rho_{\rm e}$, where it is assumed that the angle θ_{kV} does not vary significantly between the ion and electron scales. The ratio between the two break frequencies yields

$$\frac{f_{\rm be}}{f_{\rm bi}} \cong \frac{f_{\rho e}}{f_{\rho {\rm i}}} = \frac{\rho_{\rm i}}{\rho_{\rm e}} = 43\sqrt{\frac{T_{\rm i}}{T_{\rm e}}}. \quad (2)$$

On the other hand, if dispersive modes are present at electron scales then the electron breakpoint will correspond to a higher frequency in the spacecraft frame, while the ion break will still correspond to $f_{\rho{\rm i}}$. This is shown in Figure 1(a) for the case of the whistler mode at different angles of propagation. In this case Equation (2) will not be fulfilled. More specifically, if the two rhs terms of Equation (1) are positively defined one obtains

$$\frac{f_{\rm be}}{f_{\rm bi}} \gg 43\sqrt{\frac{T_{\rm i}}{T_{\rm e}}}. \quad (3)$$

Typically, in the solar wind, for quasi-parallel whistler modes one obtains $f_{\rm be}/f_{\rm bi} \sim f_{\rm ce}/f_{\rho{\rm i}} \sim 140 > 43$ (assuming $f_{\rm ce} \sim 200$ Hz, $f_{\rho{\rm i}} \sim 0.5$ Hz and $\beta_{\rm i} \sim \beta_{\rm e} \sim 1$ and $f_{\rm be} \sim f_{\rm de}$ estimated from Equation (4) below). From this discussion it appears that Equation (2) can provide a quantitative test of the validity of the Taylor hypothesis at electron scales. In Figures 1(b) and (c) one can note additionally the effect of dispersion on the slopes of the energy spectra observed on board the spacecraft: shallower spectra are obtained when the dispersive term $\omega_{\rm plas}$ dominates over the Doppler shift on the rhs of Equation (1) (Klein et al. 2014). A complete study of this effect will be published elsewhere.

2.2. Spectra Fitting Method

Since the test is based on estimating the ratio between two spectral breaks, which is a difficult task to achieve in spacecraft data, we discuss in this section the iterative method that we

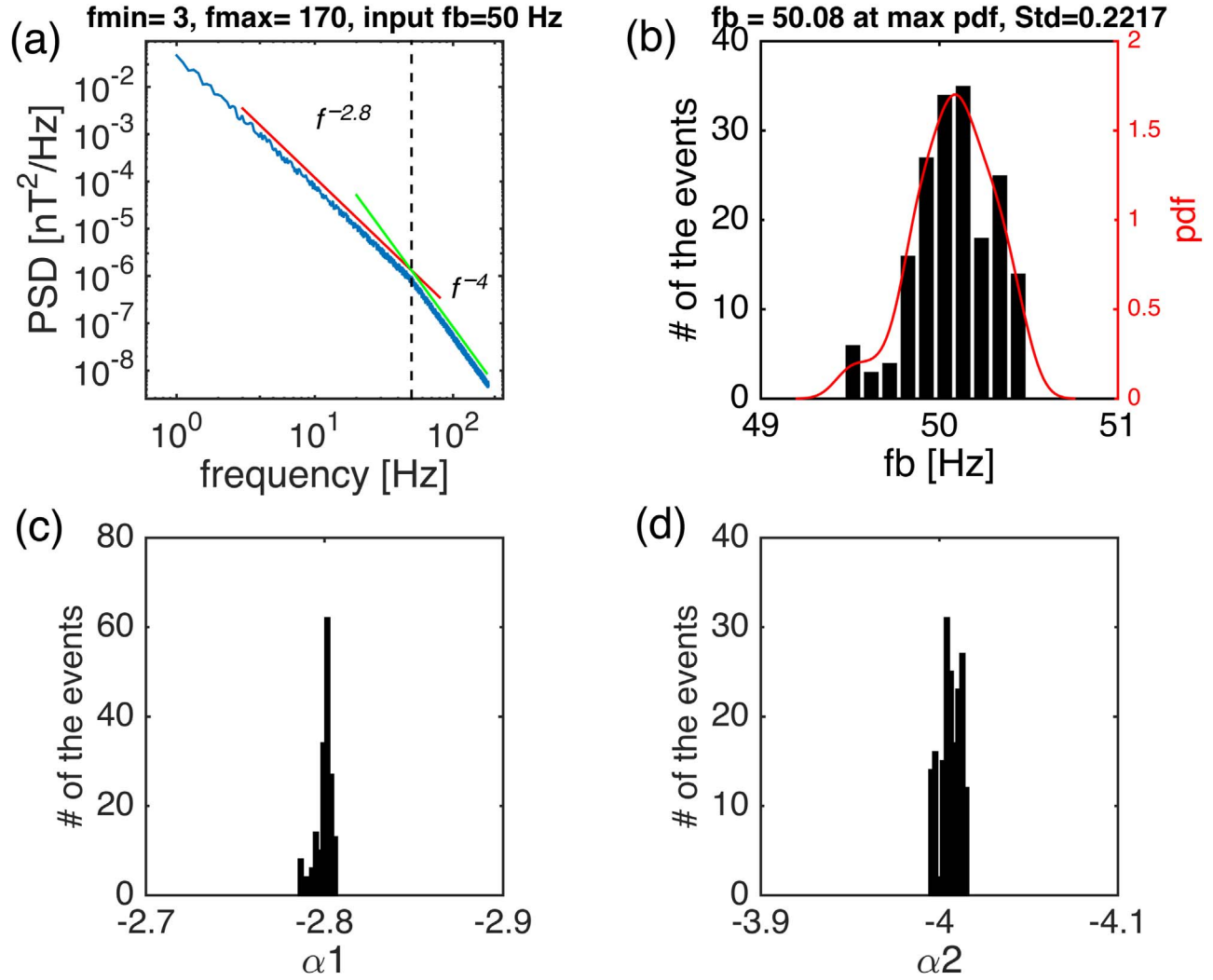

Figure 2. (a) Synthetic double power-law spectrum with 20% random noise, and (b) histogram and the probability distribution function (PDF) of the spectral break f_b resulting from the slopes at sub-ion (c) and sub-electron (d) scales.

developed to obtain the best estimate of the spectral breaks, i.e., obtained with the least statistical errors.

The method uses the double power-fitting function to obtain the spectral break f_b by the intersection of two straight lines that fit each of the sub-ion and sub-electron ranges plotted on log–log scales (see Sahraoui et al. 2013; Duan et al. 2018). To define the fitting ranges, lower (f_{min}) and upper (f_{max}) bounds are first defined to delimit the full range of frequencies to fit. Then, two initial frequencies, $f_1(i = 0)$ and $f_2(i = 0)$, defining the range that is assumed to contain the spectral break, are chosen (i.e., $f_b \in [f_1, f_2]$). Note that the choice of f_1 and f_2 can be arbitrary because the method is iterative. However, to reduce the convergence time of the algorithm, a visual inspection of the spectrum to identify the approximate location of the break can be used. A first determination of the break can be obtained from the intersection of the two straight lines fitting the ranges $[f_{min}, f_0]$ and $[f_0, f_{max}]$, where f_0 is a given frequency in the interval $[f_1, f_2]$ (see Figure 2(a)). Varying f_0 within the interval $[f_1, f_2]$ allows us to construct the PDF (probability distribution functions) of the slopes of the two power-law fits and the resulting spectral break f_b. The maximum of the PDF provides the retained value of the spectral break $f_b(i = 0)$ (see Figure 2(b)), while the standard deviation yields the corresponding statistical errors. An iterative method is further used by varying the frequencies f_1 and f_2 through the formulas by $f_1(i+1) = f_1(i)+\delta f$ and $f_2(i+1) = f_2(i) - \delta f$, where $\delta f = 0.8^*\min([\mathrm{abs}(f_b(i) - f_1(i))\ \mathrm{abs}(f_2(i) - f_b(i))])$, i.e., the minimum frequency between absolute value of $f_b(i) - f_1(i)$ and absolute value of $f_2(i) - f_b(i)$. When the absolute value of $(f_b(i+1) - f_b(i))/f_b(i)$ is smaller than 0.001, the iteration stops. Through this choice, we ensure reducing the volatility in the determination of the spectral breaks. The method is first tested on a synthetic spectrum that has a double power law, before it is used on real data. The results are shown in Figure 2 for the double power law with a 20% amplitude of random noise. One can see that the method captures both the slopes of the spectrum and the spectral break. An application of the method to a real case study is shown in Figure 3. These results indicate the robustness of our method to determine the slopes of the spectra and the corresponding spectral break.

3. Results

After validating the method as explained above, we apply it to the same data set as in Sahraoui et al. (2013) measured in the

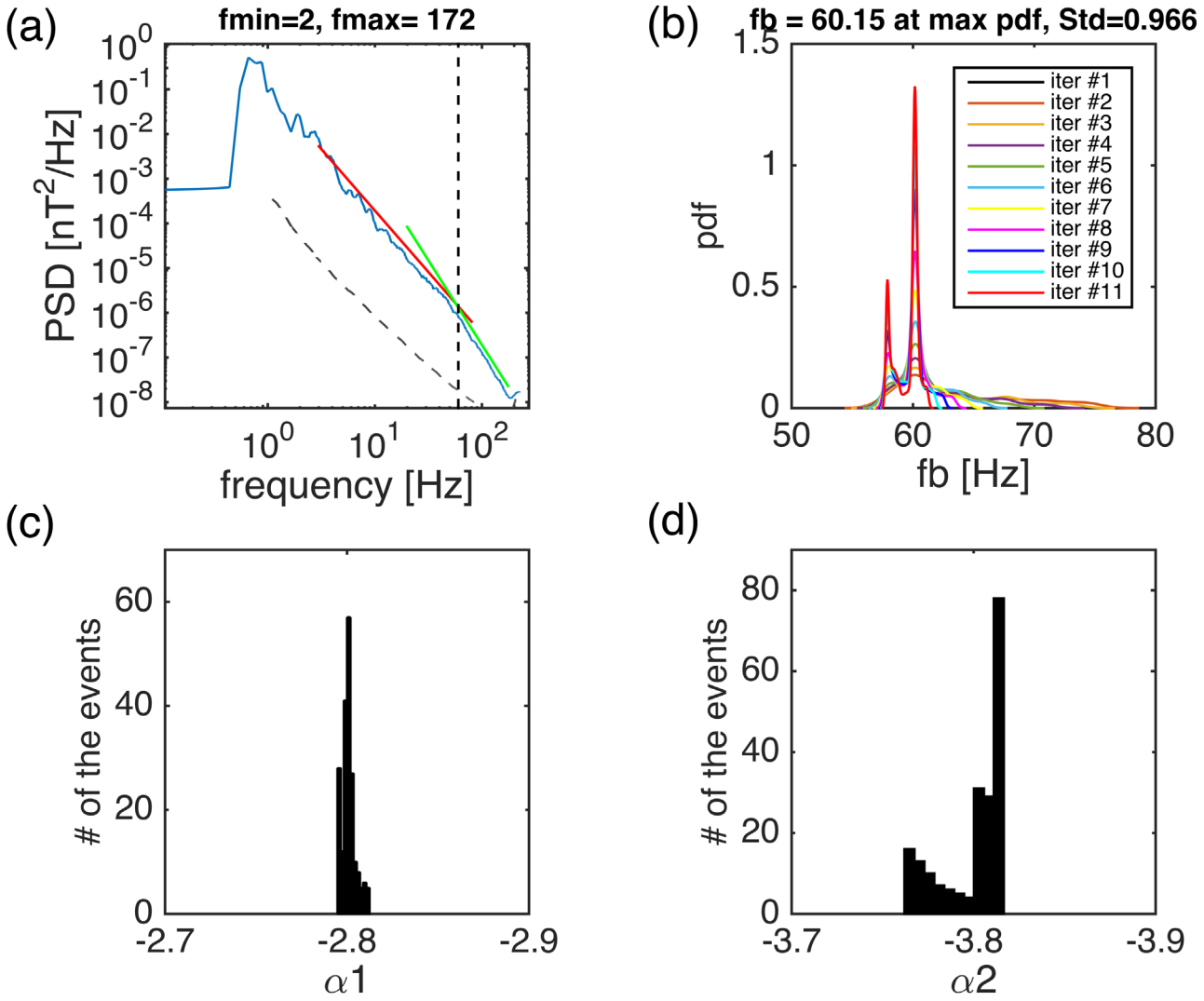

Figure 3. (a) Spectrum from real data measured by *Cluster* from 2004 January 10 about 06:18 UT on, and (b) PDF of the spectral break f_b for 11 iterations (f_b and the standard deviation retained are from the last iteration). (c) and (d) Histograms of the resulting slopes at sub-ion and sub-electron (d) scales for the last iteration. The dashed gray curve in (a) is the sensitivity of the STAFF instrument.

free-streaming solar wind. The magnetic field fluctuations in the frequency range [1, 180] Hz were measured by the STAFF/SC (Cornilleau-Wehrlin et al. 2003); the electron and ion plasma data were measured respectively by the PEACE (Gustafsson et al. 1997) and the CIS/HIA instruments (Rème et al. 2001). In addition to the data used in Sahraoui et al. (2013), we used the magnetic field data measured by the FGM instrument (Balogh et al. 2001) to cover the inertial range $\sim[10^{-3}, 1]$ Hz. Merging the STAFF/SC and the FGM data near 1 Hz allows us to cover about five decades in frequency that span the inertial, sub-ion, and sub-electron scales (e.g., Sahraoui et al. 2009). However, as shown in Sahraoui et al. (2013), the electron physics may vary very rapidly (within a few seconds) compared to the MHD or ion-scale physics. In particular, it has been shown that the frequency of the electron break can vary over a few seconds, and that computing the spectra over much longer time intervals results in smoothing out the spectral breaks, which yields curved-like spectra. This led us to performing a statistical study of the break frequencies over short intervals of ∼10 s. On the other hand, to capture the inertial range and the ion breaks, longer time intervals are required (a minimum of a few minutes is needed to capture part of the inertial range). To overcome this difficulty, we analyzed 15 data sets of 10 minute duration from the *Cluster* mission (Sahraoui et al. 2013), each of which includes several spectra computed over ∼10 s that showed clear breakpoints at the electron scale. We assume that the ion break frequency does not vary within the interval of 10 minutes. An example of the analyzed spectra is shown in Figure 4. For each individual spectrum computed over 10 s we estimated the ratio f_{be}/f_{bi}, where f_{bi} is the break observed on a spectrum computed over 10 minutes. The statistical results are shown in Figure 5. Within the assumptions described above all the points (black dots) that lie far from the curve $\frac{f_{be}}{f_{bi}} = 43\sqrt{\frac{T_i}{T_e}}$ (dashed line) do not strictly satisfy the Taylor hypothesis. Under the same assumptions, the points that are below the dashed line satisfy the condition $\frac{f_{be}}{f_{bi}} < 43\sqrt{\frac{T_i}{T_e}}$ and can be observed only if the two rhs terms of Equation (1) are not positively defined. Figure 5(a) shows the same results when a single spectrum is considered for the

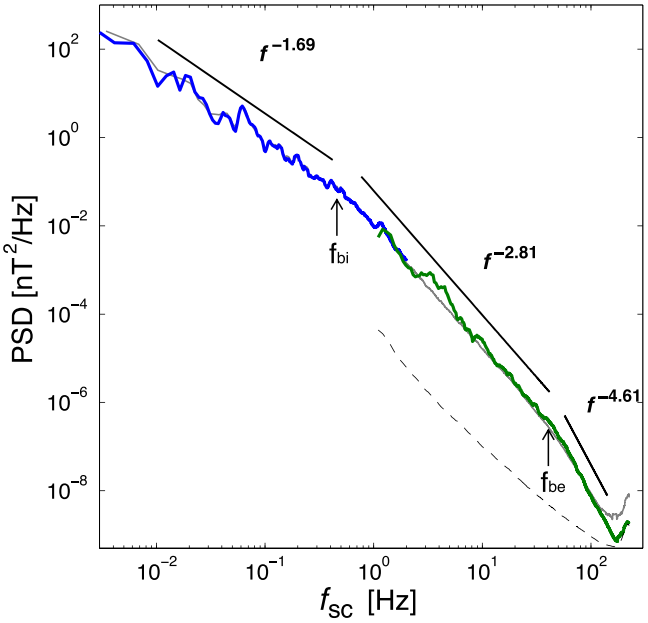

Figure 4. Example of the magnetic field spectra measured from 16:00 to 16:10 UT on 2003 March 3. The solid gray curve is the FFT spectrum calculated from the merged STAFF and FGM data, while the blue curve shows the spectrum from the FGM instrument, and the green curve is the spectrum of 9.1 s from STAFF instrument. The dashed gray curve is the sensitivity of STAFF instrument. The arrows indicate the spectral breakpoints.

whole 10 minute interval. Considering that the spectral breaks get smoothed out in this case (see Figure 9 in Sahraoui et al. 2013) we used the hybrid (power law and exponential) function $Af^{-\alpha}\exp(-f/f_d)$ introduced in Alexandrova et al. (2012) to fit the spectra computed over 10 minutes. In this model the "dissipation" frequency f_d plays the role of the frequency f_{be}. The ratios between f_d and f_{bi} shown in Figure 5(a) (magenta diamonds) indicate some spread away from the curve of the equation $\frac{f_{be}}{f_{bi}} = 43\sqrt{\frac{T_i}{T_e}}$ (dashed line). However, this spread is less important than that given by the individual ratios f_{be}/f_{bi} given by the break model, meaning that the Taylor hypothesis is less violated in this case. This is expected since time-averaging reduced the volatility of the spectral breaks.

In order to quantify the departure from the Taylor hypothesis reported in Figure 5(a), i.e., to estimate the ratio $\omega_{pla}/\omega_{Dopp} = \omega_{pla}/\boldsymbol{k}\cdot\boldsymbol{V}_f$, we used an empirical model based on the dispersion relation of the whistler mode that is assumed to cause the spectral breaks (Lacombe et al. 2014), and that is more likely to violate the Taylor hypothesis than the oblique KAWs (Klein et al. 2014). The dispersion relation of the used whistler mode used is given by Saito et al. (2010):

$$\omega_{pla} = \frac{k^2\cos\theta_{kB}c^2/\omega_{pe}^2}{1+(1+\sqrt{\beta_e})(k^2c^2/\omega_{pe}^2)}\omega_{ce}, \quad (4)$$

where k, θ_{kB}, c, ω_{pe}, β_e, and ω_{ce} are respectively the wave vector, the angle between the wave vector and the ambient magnetic field, the speed of light, the electron plasma frequency, the electron plasma beta, and the electron cyclotron frequency.

Figure 6 shows that the dispersion relation given by Equation (4) follows the fast (magnetosonic) mode for small propagation angles, and the intermediate mode (i.e., the extension into high frequencies of the shear Alfvén mode) for high oblique angles (close to 90°) derived from the two-fluid theory (see Sahraoui et al. 2012 and Zhao 2015 for a complete discussion of these properties). The dispersion relation of Equation (4) is used to infer the propagation angles and the ratios $\omega_{pla}/\omega_{Dopp}(\omega_{Dopp} = \boldsymbol{k}\cdot\boldsymbol{V}_f)$ at the scale $k\rho_e = 1$ of the whistler modes that are consistent with the observed ratios f_{be}/f_{bi} shown in Figure 5(b). We considered the flow speed measured on board *Cluster* for each time interval of 10 minutes and assumed an angle $\theta_{kV} = 45°$, which is consistent with the results reported in Sahraoui et al. (2010a, 2010b) using the k-filtering technique on the *Cluster* data.

Using the dispersion relations (4) and the plasma parameters measured between 16:00 and 16:10 UT on 2003 March 3 ($B = 12$ nT, $n_e = 10\,\mathrm{cm}^{-3}$, $\beta_e = 0.4$, and $V_f = 410\,\mathrm{km\,s}^{-1}$) we deduced the propagation angles corresponding to the ratios $\omega_{pla}/\omega_{Dopp} \sim 0.1$, 1.0, and 2.0 for the wave vector $k = 1/\rho_e$. The obtained angles are respectively 88°.6, 75°, and 58°.7, and the corresponding dispersion relations are those given in Figure 1(a). It is worth noting that even for relatively high oblique propagation angles ($\theta_{kB} = 75°$), the two rhs terms of Equation (1) are of the same order, i.e., $\omega_{pla}/\omega_{Dopp} = 1$, meaning that the Taylor hypothesis fails in this case (the error in estimating the frequency would then be 100%). The error drops down to reasonable values ∼10% or smaller (i.e., $\omega_{pla}/\omega_{Dopp} < 0.1$) only at very high oblique angles, $\theta_{kB} = 88°.6$.

Figure 5(b) shows that the observed ratios of f_{be}/f_{bi} are consistent with the estimated values $-0.5 < \omega_{pla}/\omega_{Dopp} < 1$ derived from our model based on the averaged parameters of each event, which correspond to propagation angles $41° < \theta_{kB} < 112°$. The events that had $|\omega_{pla}/\omega_{Dopp}| \leqslant 0.1$, i.e., those for which the Taylor assumption would be strictly valid at electron scales (with an error ∼10%), represented only 20% of the total analyzed intervals, and would correspond to whistler modes with propagation angles $\theta_{kB} \leqslant 85°$. This percentage rises up to 68% if the validity condition of the Taylor hypothesis is relaxed to $|\omega_{pla}/\omega_{Dopp}| \leqslant 0.5$, which would correspond to modes with propagation angles $68° \leqslant \theta_{kB} \leqslant 112°$. These results suggest the possible existence in our data of fluctuations that have phase speeds near $k\rho_e \sim 1$, comparable to the solar wind speed.

4. Discussion

The validity test of the Taylor hypothesis discussed above is based on several assumptions that need to be discussed. First, this test assumes that the spectral breaks occur near ρ_i and ρ_e, which is still an unsettled question. At ion scales, the breaks could occur at the cyclotron resonance scale (Bruno & Trenchi 2014) or at the ion inertial length (resp. Larmor radius) at low (resp. high) plasma beta (Bourouaine et al. 2012; Chen et al. 2014). Other authors suggested that none of the scales are relevant (Perri et al. 2010). At electron scales, Sahraoui et al. (2013) and Huang et al. (2014) found a higher correlation between the spectral breaks with the electron gyroscale than with the electron inertial length. If the relevant scales are d_i and d_e, there will be no change to Equation (2) other than dropping off the term T_i/T_e. As can be seen in Figure 5, the statistical results remain generally valid. However, if the breaks occur at different characteristic scales,

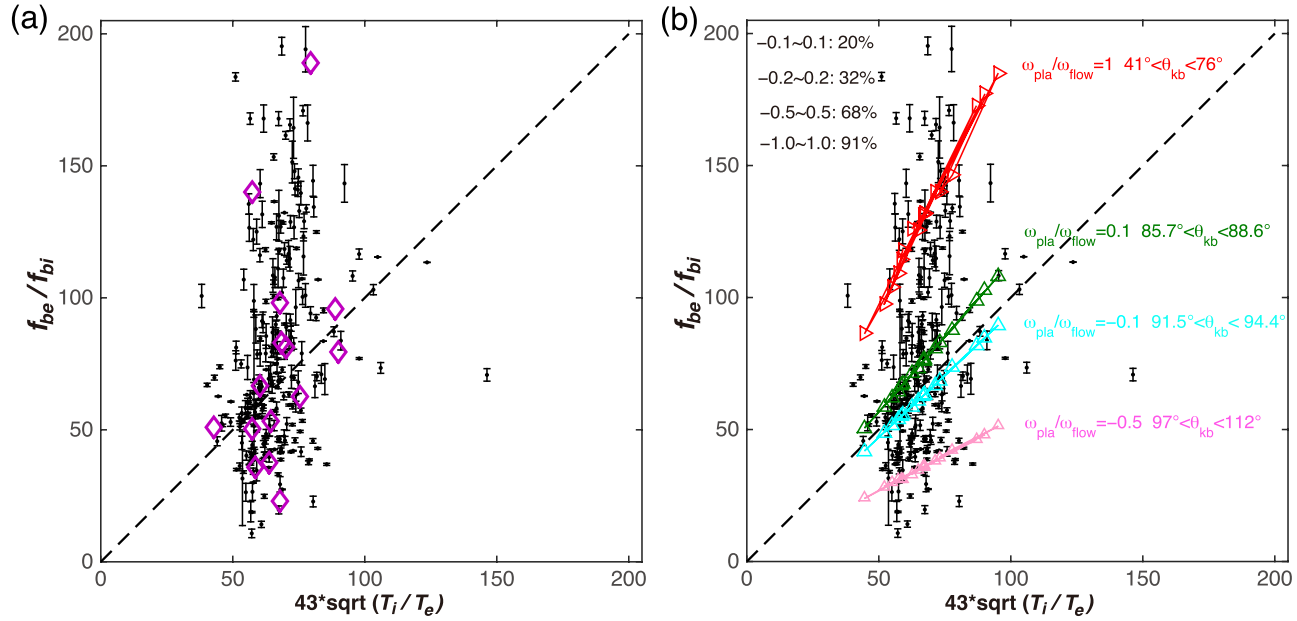

Figure 5. (a) Observed ratios of the breakpoint frequencies f_{be} and f_{bi} as a function of $43\sqrt{\frac{T_i}{T_e}}$ (black dots). The magenta diamonds represent the ratios between f_d and f_{bi} using the hybrid model to fit the spectra (see the text). (b) The magenta, cyan, green, and red triangles show the values −0.5, −0.1, 0.1, and 1 of $\omega_{pla}/\omega_{Dopp}$ at ρ_e deduced from Equation (1) and the measured solar wind parameters. The ranges of θ_{kB} correspond to the variations of θ_{kB} for all events when the values −0.5, −0.1, 0.1, and 1 of $\omega_{pla}/\omega_{Dopp}$ at ρ_e respectively. The dashed lines in (a) and (b) represent the equality $\frac{f_{be}}{f_{bi}} = 43\sqrt{\frac{T_i}{T_e}}$.

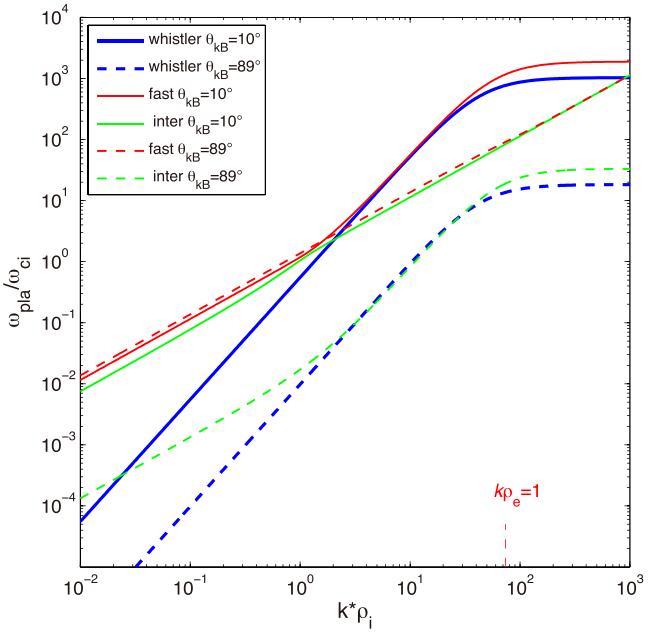

Figure 6. Comparison between the dispersion relations of the kinetic whistler mode (thick solid and dashed lines) derived in Saito et al. (2010) and the linear solutions from two-fluid theory (thin solid and dashed lines) at different propagation angles based on the averaged plasma parameters measured between 16:00 and 16:10 UT on 2003 March 3.

e.g., ρ_i and d_e (we will not discuss here the theoretical foundations of such a possibility), then Equation (2) will be modified by a factor $\sqrt{\beta_i}$ or $\sqrt{\beta_e}$. In the present statistical study β_i varies within the interval $\sim$[0.5, 4], meaning that a factor $0.7 \leqslant \sqrt{\beta_i} \leqslant 2$ should be considered in the spread observed in Figure 5 but only for a small number of events. This is because the bulk of the distribution of β_i is near the value $\sim$1 (see Figure 2 in Sahraoui et al. 2013), which implies that $\rho_i \sim d_i$ and the previous results would not change significantly (in fact only 6% of the total events have either $\sqrt{\beta_i} < 0.5$ or $\sqrt{\beta_i} > 1.5$). Even when different uncertainties in the test method are considered and the criterion of the validation of the Taylor hypothesis at the electron scale are relaxed to $|\omega_{pla}/\omega_{Dopp}| \leqslant 0.5$, 32% of the studied intervals would violate the Taylor hypothesis.

Another limitation that should be considered is that the spectral breaks may not strictly speaking occur at ρ_i or ρ_e but rather near those scales. If we assume that the breaks occur at the scales $\alpha_1\rho_i$ and $\alpha_2\rho_e$, Equation (2) remains valid as far as $\alpha_1 \sim \alpha_2$. If the two constants are different (even by a factor of $\sim$2–3), then again this will introduce an intrinsic spread in the plot of Figure 5 that would not be caused by the violation of the Taylor hypothesis.

Despite these caveats, the test presented here gives a quantitative check of the validity of the Taylor hypothesis at electron scales in space plasmas, but the conclusions should be considered within these various caveats. In the absence of multi-spacecraft missions with separations of the order of the electron scale ρ_e in the solar wind, the present test presents a good alternative to quantifying the relative importance of the Doppler shift with respect to the wave frequency in the plasma rest frame. This test will be useful for the analysis of upcoming *Parker Solar Probe* and *Solar Orbiter* data. Finally, note that recent works have emphasized the possibility of violating the Taylor hypothesis in solar wind measurements (Matthaeus et al. 2016) and the possibility of using the shape of the measured spectrum to investigate that violation (Bourouaine & Perez 2018).

5. Summary

The Taylor hypothesis is usually used in the solar wind turbulence to infer wavenumber spectra from frequency spectra

because the characteristic phase speeds in the solar wind ($V_A \sim C_s < 100\,\mathrm{km\,s^{-1}}$) are much smaller than the plasma flow velocity (typically $400 \sim 600\,\mathrm{km\,s^{-1}}$). However, as the turbulence cascade approaches the electron scale, dispersive modes with phase speeds comparable to or larger than the flow speed may exist, which makes the validity of the Taylor hypothesis questionable. The test presented in Sahraoui et al. (2012), based on the assumption that the spectral breaks occur at ρ_i and ρ_e, was applied here to test the applicability of the Taylor hypothesis at electron scales in near-Earth space plasmas before future multi-spacecraft space missions with separation comparable to the electron scales could resolve unambiguously this problem. The results showed that not all events rigorously satisfy this hypothesis, implying the existence of fluctuations with non-negligible phase speeds with respect to the solar wind speed at electron scales. Using a model based on the dispersion relation of the linear whistler mode and the estimated ratios f_{be}/f_{bi} from the *Cluster* observations, we found that only 20% of the events would strictly satisfy the Taylor hypothesis ($|\omega_{pla}/\omega_{Dopp}| < 0.1$) and correspond to propagation angles $\theta_{kB} \geqslant 85^{\circ}.7$. This percentage rises up to 68% when relaxing the criterion of validity of the Taylor hypothesis to $|\omega_{pla}/\omega_{Dopp}| \leqslant 0.5$. However, the results suggesting the possible existence of fluctuations with phase speeds (near $k\rho_e \sim 1$) comparable to the solar wind speed, should be considered within the limitations of the test method discussed above. Nevertheless, the results reported here emphasize the need to consider high-frequency observations in the solar wind with some caution with respect to the validity of the Taylor hypothesis at electron scales and to the actual frequency of the fluctuations in the plasma rest frame. They also emphasize the need of a future multi-spacecraft mission with separations of the order of the electron scale $\rho_e(\sim 1$ km) in the solar wind to resolve unambiguously these important issues for turbulence and dissipation studies. The new multi-spacecraft mission Debye, proposed recently to solve electron-scale turbulence and dissipation in the solar wind, is expected to fulfill that goal.

This work was supported by LABEX Plas@Par through a grant managed by the Agence Nationale de la Recherche (ANR), as part of the program "Investissements d'Avenir" under the reference ANR-11-IDEX-0004-02, and the THESOW project funded by ANR. S.Y. Huang acknowledges the support from the National Natural Science Foundation of China under grants 41674161 and 41874191, and the Young Elite Scientists Sponsorship Program by CAST (2017QNRC001). S. H. thanks Dr. S. Saito, Dr. J. S. Zhao, Dr. J. S. He, and Dr. D. Duan for useful discussions. The data used in this work come from the ESA/*Cluster* Active Archive (CAA) and AMDA (IRAP, France).

References

Alexandrova, O., Lacombe, C., Mangeney, A., et al. 2012, ApJ, 760, 121
Bale, S. D., Kellogg, P. J., Mozer, F. S., et al. 2005, PhRvL, 94, 215002
Balogh, A., Acuna, C. M., Dunlop, M. H., et al. 2001, AnGeo, 19, 1207
Bourouaine, S., Alexandrova, O., Marsch, E., & Maksimovic, M. 2012, ApJ, 749, 102
Bourouaine, S., & Perez, J. C. 2018, ApJL, 858, L20
Bruno, R., & Trenchi, L. 2014, ApJL, 787, L24
Chen, C. H. K., & Boldyrev, S. 2017, ApJ, 842, 122
Chen, C. H. K., Boldyrev, S., Xia, Q., & Perez, J. C. 2013, PhRvL, 110, 225002
Chen, C. H. K., Leung, L., Boldyrev, S., et al. 2014, GeoRL, 41, 8081
Cornilleau-Wehrlin, N., Chanteur, G., Perraut, S., et al. 2003, AnGeo, 21, 437
Duan, D., He, J., Pei, Z., et al. 2018, ApJ, 865, 89
Gustafsson, G., Bostrom, R., Holback, B., et al. 1997, SSRv, 79, 137
Howes, G. G., Klein, K. G., & TenBarge, J. M. 2014, ApJ, 789, 106
Huang, S. Y., Hadid, L. Z., Sahraoui, F., et al. 2017, ApJL, 836, L10
Huang, S. Y., Sahraoui, F., Deng, X. H., et al. 2014, ApJL, 789, L28
Huang, S. Y., Zhou, M., Sahraoui, F., et al. 2010, JGR, 115, A12211
Huang, S. Y., Zhou, M., Sahraoui, F., et al. 2012, GeoRL, 39, L11104
Kiyani, K. H., Chapman, C., Khotyaintsev, Yu. V., Dunlop, M. W., & Sahraoui, F. 2009, PhRvL, 103, 075006
Kiyani, K. H., Chapman, C., Sahraoui, F., et al. 2013, ApJ, 763, 10
Kiyani, K. H., Osman, K. T., & Chapman, S. C. 2015, RSPTA, 373, 20140155
Klein, K. G., Howes, G. G., & TenBarge, J. M. 2014, ApJL, 790, L20
Lacombe, C., Alexandrova, O., Matteini, L., et al. 2014, ApJ, 796, 5
Matthaeus, W. H., Weygand, J. M., & Dasso, S. 2016, PhRvL, 24, 245101
Narita, Y., Glassmeier, K.-H., Sahraoui, F., et al. 2010, PhRvL, 104, 171101
Perri, S., Carbone, V., & Veltri, P. 2010, ApJL, 725, L52
Rème, H., Aoustin, C., Bosqued, J. M., et al. 2001, AnGeo, 19, 1303
Sahraoui, F., Belmont, G., & Goldstein, M. L. 2012, ApJ, 748, 100
Sahraoui, F., Belmont, G., & Rezeau, L. 2003, PhPl, 10, 1325
Sahraoui, F., Goldstein, M. L., Belmont, G., Canu, P., & Rezeau, L. 2010a, PhRvL, 105, 131101
Sahraoui, F., Goldstein, M. L., Belmont, G., et al. 2010b, P&SS, 59, 585
Sahraoui, F., Goldstein, M. L., Robert, P., & Khotyaintsev, Y. V. 2009, PhRvL, 102, 231102
Sahraoui, F., Huang, S. Y., Patoul, J. De, et al. 2013, ApJ, 777, 15
Saito, S., Peter Gary, S., & Narita, Y. 2010, PhPl, 17, 122316
Salem, C. S., Howes, G. G., Sundkvist, D., et al. 2012, ApJL, 745, L9
Tjulin, A., Pinçon, J.-L., Sahraoui, F., et al. 2005, JGR, 110, A11224
Zhao, J. S. 2015, PhPl, 22, 042115
Zhao, J. S., Voitenko, Y., Yu, M. Y., Lu, J. Y., & Wu, D. J. 2014, ApJ, 793, 107